2nd URSI AT-RASC, Gran Canaria, 28 May – 1 June 2018

DELAYED RESPONSE OF THE IONOSPHERIC WEATHER TO FIVE THE MOST POWERFUL GEOMAGNETIC SUPERSTORMS

O. Grynyshyna-Poliuga[1], T.L. Gulyaeva[2], I . Stanislawska[1], L.V. Poustovalova[2].

[1]Space Research Centre PAS, Bartycka 18a, 00-716 Warsaw, Poland: stanis@cbk.waw.pl; ogp@cbk.waw.pl
[2]IZMIRAN, Troitsk, 108840 Moscow, Russia: gulyaeva@izmiran.ru; pustoval@izmiran.ru

Abstract

This work presents results of reconstruction of the ionospheric weather during five the most intense superstorms observed since IGY (1957, 1958, 1959, 1989, 2003) with the instantaneous global maps of the F2 layer critical frequency, GIM-foF2, and the ionospheric weather index maps, GIM-Wf.

1. Introduction

The geomagnetic and ionospheric superstorms have been analyzed in literature with different criteria applied to various geomagnetic and ionospheric indices (Bell et al., 1997; Loewe and Prölss, 1997; Liu et al., 2007; Gulyaeva, 2017; Verkhoglyadova et al., 2017). To find out the ionospheric signatures of the superstorms, the instantaneous global ionospheric maps of the F2 layer critical frequency, GIM-foF2, have been produced.

Production of the instantaneous global maps of the F2 layer peak parameters (critical frequency, GIM-foF2, and peak height, GIM-hmF2) provides independent instant global presentation of the ionosphere estimated from different scales of reference station networks far from an average quiet time behavior. The proposed technique for foF2 map adjustment to the climatological ITU-R predictions appears to be very promising for investigation of the ionospheric weather in the past for few decades of ionosonde observations when none GNSS monitoring of the ionosphere existed. The results of such investigation are presented below.

2. Data analysis

Five the largest geomagnetic superstorms has occurred during six Solar Cycles (SC19 to SC24) since the International Geophysical Year (IGY), from 1957 to 2017, which are selected for the present study. We define the Storm Power with the peak absolute amplitude of index (|Xpeak|) multiplied by the storm duration Δt_s, hrs:

$$SP(X) = |Xpeak| \times \Delta t_s \quad (1).$$

Criteria for the superstorm are similar to those introduced for the intense storm onset, peak and duration which are presented in (Gulyaeva, 2017). Only these five superstorms have been observed with minimum $Dst_{min} < -400$ nT (http://wdc.kugi.kyoto-u.ac.jp/) listed in the catalog of Dst storms at http://www.izmiran.ru/ionosphere/weather/storm/. Four superstorms are observed at the extremely high solar activity near the peak of solar cycle, and one event (2003) at the moderate solar activity on the downslope from solar maximum. The geomagnetic indices are analyzed for one day before the day of superstorm peak, the day of the peak amplitude and two following days.

The W-index is introduced as a segmented logarithmic scale of the ionospheric weather for the different thresholds of change in peak plasma density NmF2 or total electron content TEC for quantifying the ionosphere variability (Gulyaeva et al., 2008). We define an intensity of global ionospheric storm by percentage occurrence Wf^+, %, of positive ionosphere storm index (W = 3, 4) and negative ionosphere storm index Wf^-, %, (W = -3, -4) relative to the total global cell number. The planetary Wfp(foF2) index or Wp(TEC) index presents weighted global average of drop between maximum positive W^+ index and minimum negative W^- index at each latitude on the globe (Gulyaeva and Stanislawska, 2008). The planetary Wfp index is produced for each hourly Wf map for the month of superstorm. Superposed epoch analysis of the ionospheric Wfp index is made for the five extreme superstorms during 24 h before the Wfp peak (at the time zero $t_0 = 0$ h) and 48 h afterwards. Relevant sliding data sets of 72 h periods are extracted from the geomagnetic storm profiles to calculate the ionosphere - geomagnetic field delayed correlation and the time lag Δt, hours, of the ionospheric response delay regarding the geomagnetic storm occurrence. The delayed correlation between two variables, $C_{X/Y}(\Delta t)$ corresponds to the correlation coefficient between the variable $Y(t + \Delta t)$ and the variable $X(t)$. Similar approach has been used by Liu et al. (2007) in investigation of time delay of the ionospheric total electron content responses to geomagnetic disturbances.

3. Results

Superposed epoch analysis of the geomagnetic indices and ionospheric Wfp index is made referring to the time of Dst_{min} as zero epoch (UT hour of Dst peak given in Table 1). All geomagnetic indices and Wfp index were collected for 24 h prior to zero epoch and 48 h afterwards. Then median of five superstorm profiles of each geomagnetic index and average Wfp index have been produced. In order to identify time lag between the geomagnetic superstorms and the ionospheric superstorm, the superposed epoch analyses has been repeated with the zero epoch assigned (t_0 = 0) at Wfp_{max} as observed from the Wfp average profile. Results are illustrated in Figure 1a-e for the period from t_0 – 24 h to t_0 + 48 h: (a) Wfp index; (b) Dst index; (c) AE index; (d) aa index; (e) ap index.

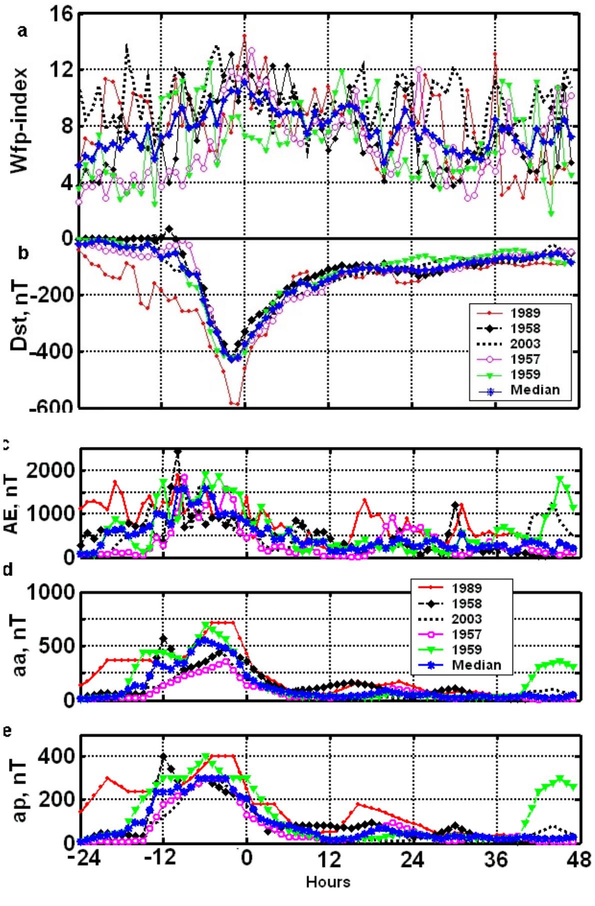

Figure 1. Results of the superposed epoch analyses for five superstorms with the geomagnetic and ionospheric indices (t_0 = 0 at Wfp_{max} of average Wfp profile): (a) Wfp index; (b) Dst index; (c) AE index; (d) aa index; (e) ap index.

The time lag Δt of the Wfp_{max} (t_0 = 0) of the average Wfp profile from the peak of each geomagnetic median profile (Dst_{min}, AE_{max}, aa_{max}, ap_{max}) is estimated and presented in Table 1. The delay of the average ionospheric response of Wfp_{max} to geomagnetic superstorm is equal to Δt = 9 h regarding AE_{max}, Δt = 6 h from aa_{max} and ap_{max}, Δt = 2 h from Dst_{min}.

Table 1

Coefficients of analytical regression between average Wfp profile and median geomagnetic superstorm profile for selected indices (X) with time lag Δt, hours, between peak of geomagnetic storm and ionospheric storm, and correlation coefficient (r_2), derived from GIM-Wf index maps.

X	A	B	C	Δt	r_2
AE/100	-0.0064	0.3339	6.5064	9	0.67
ap/100	-0.2063	1.6299	6.8000	6	0.70
aa/100	-0.0363	0.8053	7.0269	6	0.71
Dst/100	-0.1226	-1.5142	6.1977	2	-0.74

Taking the time lag Δt into account, the delayed correlation coefficient r_2 between the average Wfp profile and each median geomagnetic storm profile (shifted by time lag obtained) are also provided in Table 1. Second order regression between average Wfp profile and each (X) of four median geomagnetic storm profiles (shifted by time lag) is established with the best fit of the 2nd order polynomial:

$$Wfp = AX^2 + BX + C \quad (2)$$

The empirical regression relations obtained for the ionospheric superstorm observed with a significant delay (time lag) regarding the geomagnetic superstorms present a model which can be used for forecasting the profile of the planetary foF2 (NmF2) superstorm (Wfp index profile) if an extreme geomagnetic superstorm is captured with one or more of the geomagnetic indices.

4. Conclusions.

The intensity of the ionospheric superstorm is characterized by the planetary Wfp index derived from GIM-Wf maps which presents weighted global average of drop between maximum positive Wf^+ index and minimum negative Wf^- index at each latitude on the globe. Superposed epoch analysis of the extreme superstorms is made during 24 h before the Wfp peak (time zero t_0 = 0 h) and 48 h afterwards. It is found:

(1) The delayed correlation analysis has revealed a good resemblance between the geomagnetic and ionospheric superstorm patterns.

(2) Model relationship is established between mean Wfp profile and geomagnetic superstorm profiles demonstrating saturation of the ionospheric storm activity towards the peak of geomagnetic storm.

(3) Time lag (delay) of the ionospheric Wfp_{max} response to geomagnetic superstorm is found equal to 9 h from AE_{max}, 6 h from ap_{max} and aa_{max}, 2 h after Dst_{min} which allows model forecast of ionospheric superstorm when geomagnetic superstorm is captured with one or more of geomagnetic indices.

5. Acknowledgements

The PRIME251 foF2 instantaneous maping software are provided by SRC at http://rwc.cbk.waw.pl/. The ionosonde foF2 data and geomagnetic aa index are provided by UK Solar System Data Centre (http://www.ukssdc.ac.uk/wdcc1/data_menu.html), ionosonde foF2 data by Australian Space Weather Data Service (http://www.sws.bom.gov.au/World_Data_Centre/1/3), NICT, Japan (http://wdc.nict.go.jp/IONO/HP2009/ISDJ/index-E.html), NOAA SPIDR Server, USA (http://spidr.ionosonde.net/spidr/), IZMIRAN Ionospheric Weather service, RF (http://www.izmiran.ru/ionosphere/weather/). Geomagnetic AE, Dst and ap indices are provided by WDC for Geomagnetism, Kyoto, Japan (http://wdc.kugi.kyoto-u.ac.jp/). This study is partly supported by the Europlanet 2020 RI project funded under Horizon 2020, the EU research and innovation programme - grant agreement No 654208 and TUBITAK EEEAG 115E915 project.

6. References

1. J.T. Bell, M.S. Gussenhoven, E.G. Mullen "Superstorms" J. Geophys. Res., **102**, A7, 1997, 14,189-14,198.

2. T.L. Gulyaeva, "Ranking ICME's efficiency for geomagnetic and ionospheric storms and risk of false alarms," J. Atmos. Solar-Terr. Phys., 2017, DOI:10.1016/j.jastp.2017.07.021.

3. T.L. Gulyaeva, I. Stanislawska, M. Tomasik, "Ionospheric weather: cloning missed foF2 observations for derivation of variability index," *Ann. Geophys.*, **26**, 2008, pp. 315-321, DOI:10.5194/angeo-26-315-2008.

4. T.L. Gulyaeva and I. Stanislawska, "Derivation of a planetary ionospheric storm index," Annales Geophysicae, **26**, N.9, 2008, pp. 2645-2648.

5. J. Liu, B. Zhao, and L. Liu, "Time delay and duration of ionospheric total electron content responses to geomagnetic disturbances," Ann. Geophys., **28**, 2007, pp. 795-805.

6. C.A. Loewe and G.W. Prölss, "Classification and mean behavior of magnetic storms," J. Geophys. Res., **102**, A7, 1997, 14,209-14,213.

7. O.P. Verkhoglyadova, A. Komjathy, A.J. Mannucci, M.G. Mlynczak, L.A. Hunt, L. J. Paxton, "Revisiting Ionosphere-Thermosphere Responses to Solar Wind Driving in Superstorms of November 2003 and 2004," J. Geophys. Res. Space Phys., DOI:10.1002/2017JA024542.